# Cancer Immunoediting

## Simulating metabolic competition in the tumor microenvironment

Vedang Narain

7 December 2018

## Introduction

Immunoediting is the biological process by which the immune system alters the progression of tumor growth [1]. The ability of tumor cells to resist and circumvent the immunoediting process is commonly attributed to the development of favorable phenotypes through Darwinian evolution. The focus of this project is the computational evaluation of the hypothesis that metabolic competition for glucose at the tumor site between cancer cells and the cells of the immune system can play a significant role in the immunoediting process and affect its outcome in terms of the resultant population of tumor cells. The possible disruptive effects of cytotoxic chemotherapeutic drugs on the immunoediting process are explored as well.

### Metabolic Context

To better understand the interactions between the immune system and tumors, it is useful to consider the metabolic context in which these interactions occur. In normal tissue, lactate production occurs almost exclusively in anaerobic conditions. However, cancer cells often carry out lactic fermentation in aerobic conditions as well, yielding two molecules of ATP for every glucose molecule, resulting in an energy yield approximately 15 times less than that of aerobic respiration [2].

While this propensity for aerobic glycolysis may seem inefficient, it should be noted that the mechanism, known as ‘the Warburg effect’, produces lactate 10–100 times quicker than the complete oxidation of glucose in mitochondrial respiration, which results in a comparable rate of ATP synthesis over a given time period [3].

There are several other proposed benefits that cancer cells may reap due to the Warburg effect, chief among them being an increase in biosynthesis necessary to sustain the rapid proliferation of tumor cells. The increase in glucose production provides a carbon source for anabolic processes. Moreover, aerobic glycolysis frees up the mitochondria to produce biosynthetic enzymes, and supports biomass growth even when mitochondrial capacity is exceeded [3]. In addition, as a tumor increases in size, its supply of nutrients and oxygen can get restricted by the number of blood vessels in its environment. The secretion of lactate can compromise for this by acidifying the microenvironment to aid metastasis by altering the tumor-stroma interface [3, 4].

Therefore, we can assume that a tumor may be comprised of a metabolically heterogeneous cell population, with one subpopulation characterized by aerobic respiration and the other by aerobic glycolysis.

## Immunoediting Mechanism

The process of immunoediting features three phases. In the first phase, ‘elimination’, tumor cells are destroyed by the immune system. Surviving cells may then enter an ‘equilibrium’ phase in which editing occurs. The ‘escape’ phase represents the third and final phase of the process, in which the tumor cells circumvent the immune response and an immunosuppressive tumor microenvironment is established [6]. The conventional explanation for tumor escape has been the mutation of the constituent cells until non-immunogenic clones are developed [1].

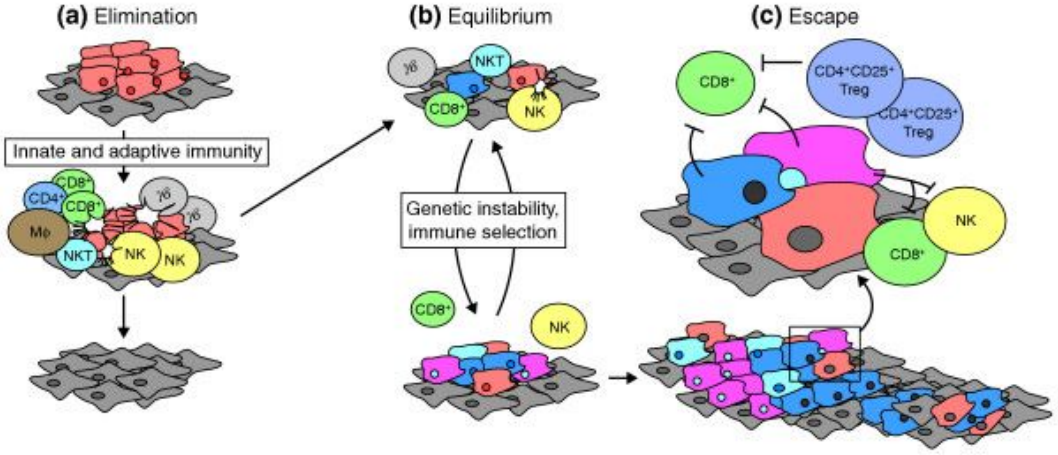


Figure 1. Phases of the immunoediting process [5]

However, competition for glucose in the microenvironment allows for another theoretical proposition. Since the cells involved in the immune response also rely on glucose for their metabolism, it would stand to reason that glucose may exist as a proliferation-limiting shared resource for both the tumor cells and the immune response, which can account for the three phases observed in the immunoediting process.

## Literature Review

This project relies primarily on the population models proposed by Irina Kareva and Faina Berezovskaya in their exposition of a predator-prey-shared resource type model of immunoediting dynamics [1]. In their model’s framework, cytotoxic lymphocytes are considered predators of the tumor cells, both of which compete for the common resource of glucose. The model proposed in the paper aims to describe a specific spatial phenomenon (Figure 2). In this scenario, a glycolytic core is formed inside a growing tumor while peripheral cells continue to employ aerobic metabolism.

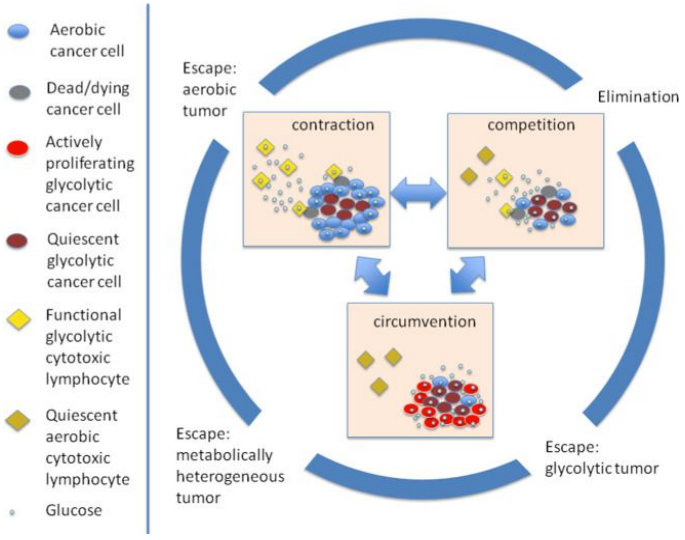


Figure 2. Metabolism-driven tumor escape [1]

The proposed system is described by a set of four differential equations (Figure 3). The first two equations represent the aerobic and glycolytic subpopulations of the tumor, while the third equation represents the amount of glucose in the system. The final equation describes the population of cytotoxic immune cells in the microenvironment. Of particular interest to this project are the two coefficients influencing immune stimulation and natural decay since they can be influenced by immunotherapy and chemotherapy respectively.

$$\frac{dT_a}{dt} = \underbrace{r_a T_a(t)\frac{G(t)}{\xi_T + b_T G(t)}}_{\text{glucose dependent growth}} - \underbrace{e_a \frac{T_a(t)I(t)}{I + s(T_a(t)+T_g(t))}}_{\text{ratio–dependent death by CTLs}} - \underbrace{\mu_a T_a(t)}_{\text{natural death}}$$

$$\frac{dT_g}{dt} = r_g T_g(t)\frac{G(t)}{\xi_T + b_T G(t)} - e_g \frac{T_g(t)I(t)}{I(t) + s(T_a(t)+T_g(t))} - \mu_g T_g(t)$$

$$\frac{dG}{dt} = \underbrace{(G_0 - \mu_G G(t))}_{\text{natural G inflow/outflow}} \underbrace{-(d_a T_a(t) + d_g T_g(t))\frac{G(t)}{\xi_T + b_T G(t)}}_{\text{G consumed by the tumor}}$$

$$- \underbrace{d_I I(t)\frac{G(t)}{\xi_I + b_I G(t)}}_{\text{G consumed by immune cells}}$$

$$\frac{dI}{dt} = \underbrace{(i_0(T_a(t)+T_g(t))}_{\text{systemic immune stimulation}} - \underbrace{\mu_I I(t))}_{\text{natural decay}}$$

$$+ \underbrace{r_I I(t)\left(\frac{G(t)}{\xi_I + b_I G(t)}\right)\left(\frac{I(t)(T_a(t)+T_g(t))}{I(t) + s(T_a(t)+T_g(t))}\right)}_{\text{cell expansion stimulated by debris from previously killed tumor cells and modulated by glucose}}$$

Figure 3. Proposed set of equations describing metabolic competition [1]

Although these mathematical equations adequately describe the competitive relationships between the four species in a metabolic context, they do not incorporate the spatial characteristics of the biological occurence exhibited in Figure 2. Therefore, a more generalized representation of a microenvironment that can be adequately described by these equations is shown in Figure 4.

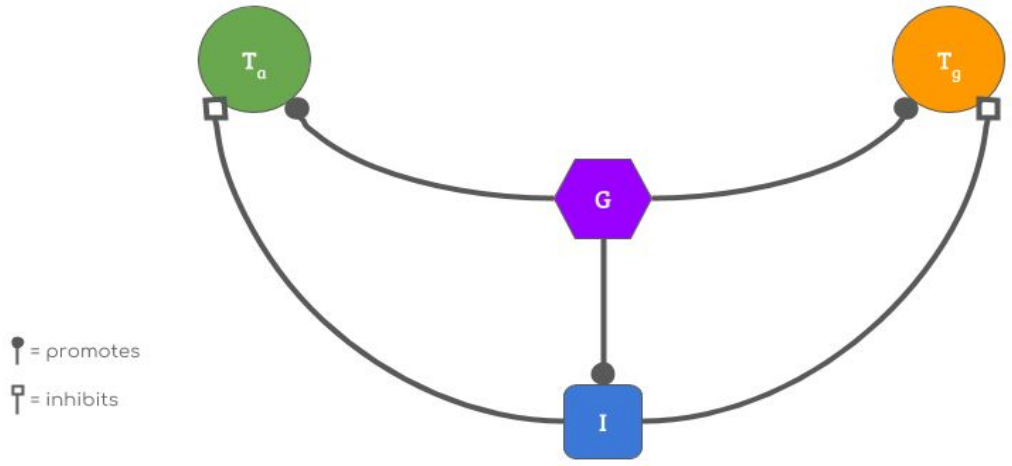


Figure 4. Generalized topological schematic of direct interactions

While the network in Figure 4 appears significantly simpler than the representation in Figure 2, a number of complex effects can be inferred from the direct relationships between $T_a$ (aerobic tumor cells), $T_g$ (glycolytic tumor cells), $G$ (glucose), and $I$ (immune system cells). For instance, although $T_a$ and $T_g$ have no direct metabolic relationship, the two species both compete for $G$. Thus, they inhibit each other's proliferation. However, since the two tumor cell populations compete for the same resource as $I$, they inhibit the proliferation of $I$. Since $I$ negatively affects the populations of tumor cells, the two subpopulations of tumor cells also assist each other's growth.

The need for simulations is apparent since the outcome of the complex interactions within the model cannot easily be inferred from visual inspection alone.

# Methods

The Python (3.5) programming language was utilized in the Spyder (3.1.4) IDE in conjunction with the Tellurium (2.1.3) environment to develop a model of the dynamic system. The equations outlined in Figure 3 were applied to describe the abstracted network (Figure 4), with some modifications made to account for the effect of chemotherapy.

## Modeling Chemotherapeutic Intervention

The fact that general chemotherapy results in the death of both cancer cells and immune cells can be represented by a topological network abstraction (Figure 5).

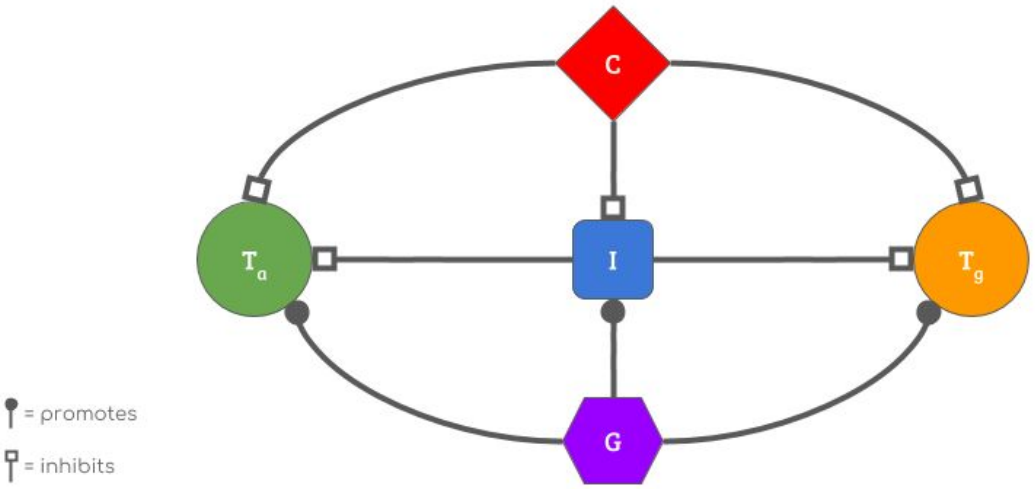


Figure 5. Topological schematic accounting for chemotherapeutic intervention

The set of equations used to describe the original model can be modified to account for the presence of a cytotoxic chemical (*C*) in the microenvironment.

$$\frac{dT_a}{dt} = r_a T_a(t)\frac{G(t)}{\xi_T + b_T G(t)} - e_a \frac{T_a(t) I(t)}{I(t) + s\left(T_a(t) + T_g(t)\right)} - \mu_a T_a(t)$$

$$\frac{dT_g}{dt} = r_g T_g(t)\frac{G(t)}{\xi_T + b_T G(t)} - e_g \frac{T_g(t) I(t)}{I(t) + s\left(T_a(t) + T_g(t)\right)} - \mu_g T_g(t)$$

$$\frac{dG}{dt} = \left(G_0 - \mu_G G(t)\right) - \left(d_a T_a(t) + d_g T_g(t)\right)\frac{G(t)}{\xi_T + b_T G(t)} - d_I I(t)\frac{G(t)}{\xi_I + b_I G(t)}$$

$$\frac{dI}{dt} = \left(i_0\left(T_a(t) + T_g(t)\right) - \mu_{I_C} I(t)\right) + r_I\left(\frac{k_I I(t)}{k_I + I(t)}\right)\frac{G(t)}{\xi_I + b_I G(t)}\left(\frac{I(t)\left(T_a(t) + T_g(t)\right)}{I(t) + s\left(T_a(t) + T_g(t)\right)}\right)$$

$$\frac{dC}{dt} = -\mu_C C$$

$$\frac{d\mu_{I_C}}{dt} = \mu_{I_C} C + \frac{\mu_I - \mu_{I_C}}{p}$$

Figure 6. Accounting for chemotherapeutic dosage (modifications indicated in blue)

The equation describing the dynamics of the immune system cell population is modified to introduce a new coefficient of elimination, which takes into account both the natural death rate and the death rate induced by chemotherapy (Figure 7). The decay of the chemotherapeutic chemical species is modulated by the coefficient $\mu_C$. The recovery period for immune cells is denoted by $p$.

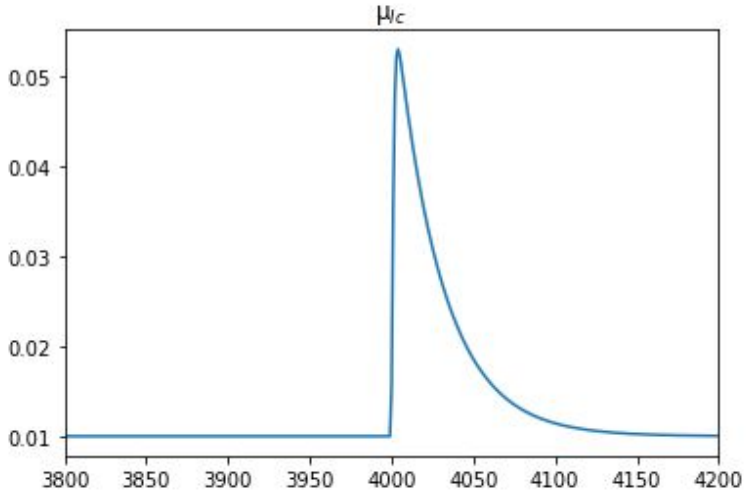


Figure 7. The value of the coefficient of elimination decays as the amount of $C$ decreases ($C$ introduced at time = 4000 days)

**Assumptions**

Defining a topological model to isolate metabolic interactions involved several assumptions.

1. Tumor cells replicate faster than immune cells.
2. The supply of glucose is continuous, limited, and induces competition.
3. The supply of oxygen is sufficient to avoid competition.
4. Glycolytic tumor cells proliferate faster than aerobic tumor cells.
5. The effects of genomic instability can be excluded; there are no non-immunogenic clones.
6. Chemotherapy eliminates 90% of the tumor cell population, and all cancer cells are equally affected.
7. The initial tumor cell population is 90% glycolytic and 10% aerobic.
8. The permeating effects of lactic acid can be excluded.
9. The tumor is spatially bounded and unable to metastasize through the bloodstream.

# Results

The results of the simulations were visualized graphically, with the x-axis representing time in units of days, and the y-axis representing populations. A dotted vertical line demarcates the 30-year mark. Since the median age of cancer diagnosis in the USA is 66 years and the average life expectancy is 79 years, this mark allows us to visualize a reasonable period beyond which the resurgence of cancer may be ignored [7, 8]. The results of the initial simulations implemented in this project are displayed to the right of the figures provided in the original paper.

**Simulating Immunotherapy**

Variations of $i_0$ simulate the effects of different immunological changes. For example, an increase in $i_0$ could represent the administration of immunotherapy, while a lowered value of $i_0$ could represent the onset of an immunodeficiency disease.

Running the first simulation with $i_0 = 0.00020$ mm$^3$/day (Figure 8) shows that the tumor manages to achieve the 'escape' phase of immunoediting with little difficulty.

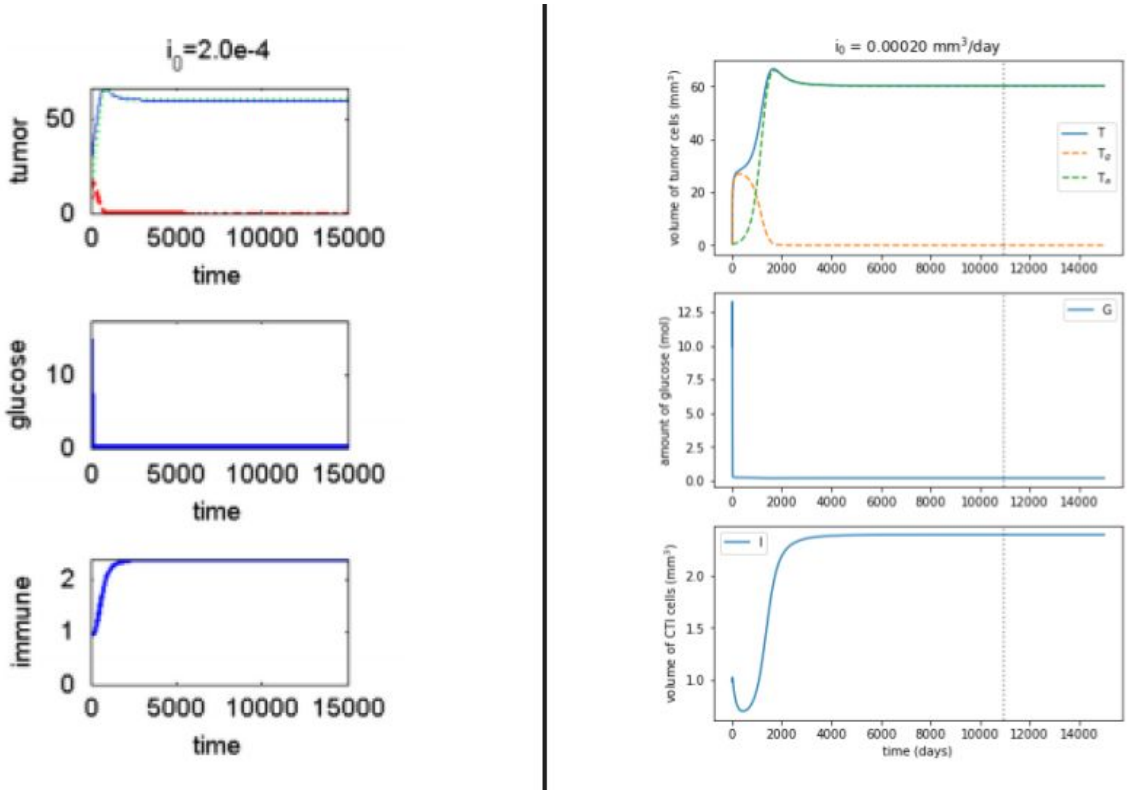


Figure 8. Results of simulation with $i_0 = 0.00020$ mm$^3$/day [1]

The amount of glucose drops rapidly, falling to a non-zero value in approximately a month due to the presence of a large population of aerobic tumor cells. The initial population of *I* falls as the amount of glucose available decreases and subsequently recovers, but is unable to check tumor growth. The scarcity of glucose also inhibits the proliferation of glycolytic tumor cells.

Upon increasing the immune stimulus, the tumor enters the 'equilibrium' phase of immunoediting (Figure 9). Cyclical dynamics that resemble predator-prey populations in an ecosystem can be observed. A closer look at the oscillations reveals that the low value of *G* inhibits the growth of glycolytic cells. Simultaneously, the immune system is stimulated by the presence of aerobic tumor cells that are subsequenly eliminated. Once the population of $T_a$ reaches a minimum, *I* falls due to a lack of immune stimulus.

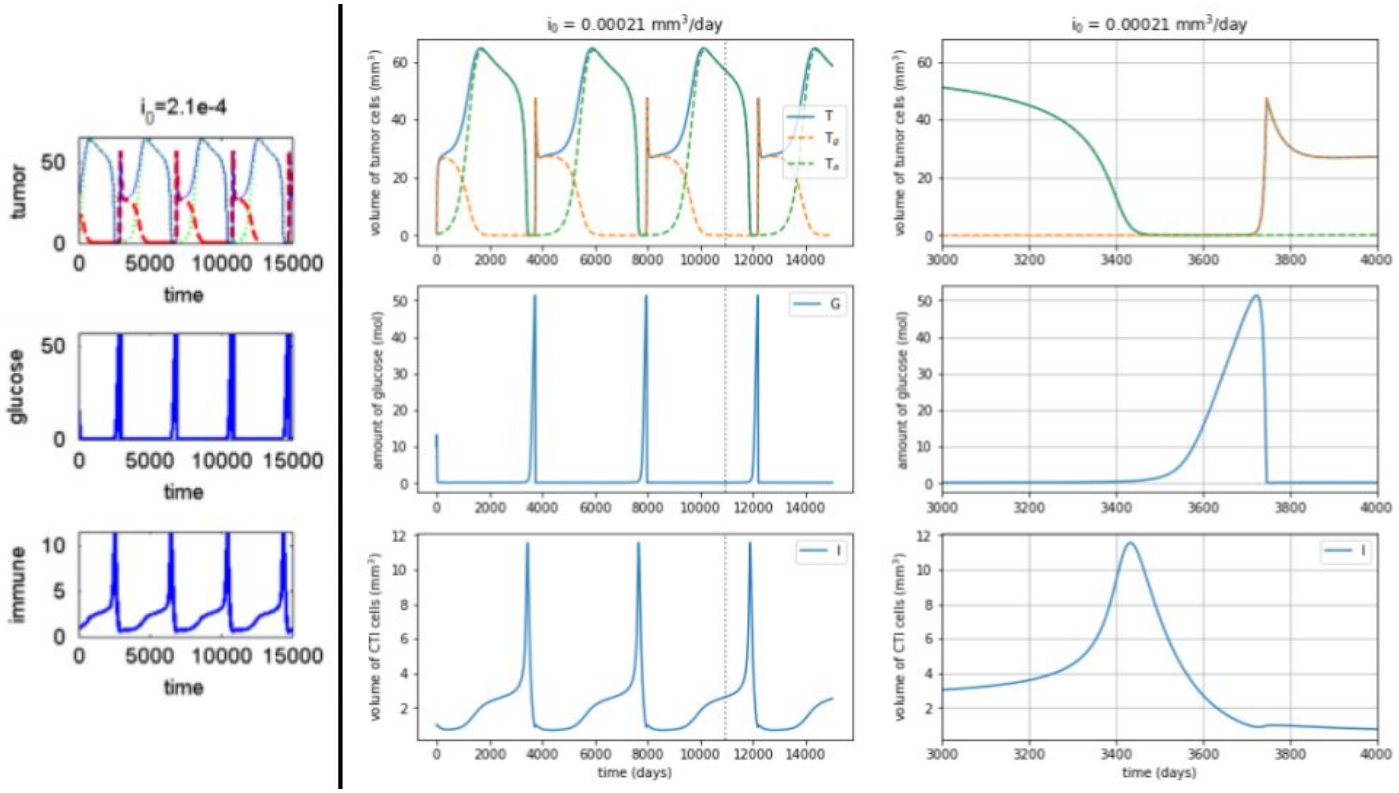


Figure 9. Results of simulation with $i_0 = 0.00021$ mm$^3$/day [1]

The absence of glucose consumption in the microenvironment allows glucose to accumulate in the system. In turn, this allows the population of $T_g$ to rise as well. However, the resultant drop in glucose levels inhibits the growth of the glycolytic cell population and allows $T_a$ to increase in the absence of an immune response. Once the immune response commences again, the cycle is repeated.

While this form of cyclical equilibrium prevents the tumor from overwhelming the immune system, it is far from clinically ideal since the overall tumor size peaks at a high value, which may have severe physiological implications.

Further increasing the immune stimulus allows for the observation of the 'elimination' phase (Figure 10).

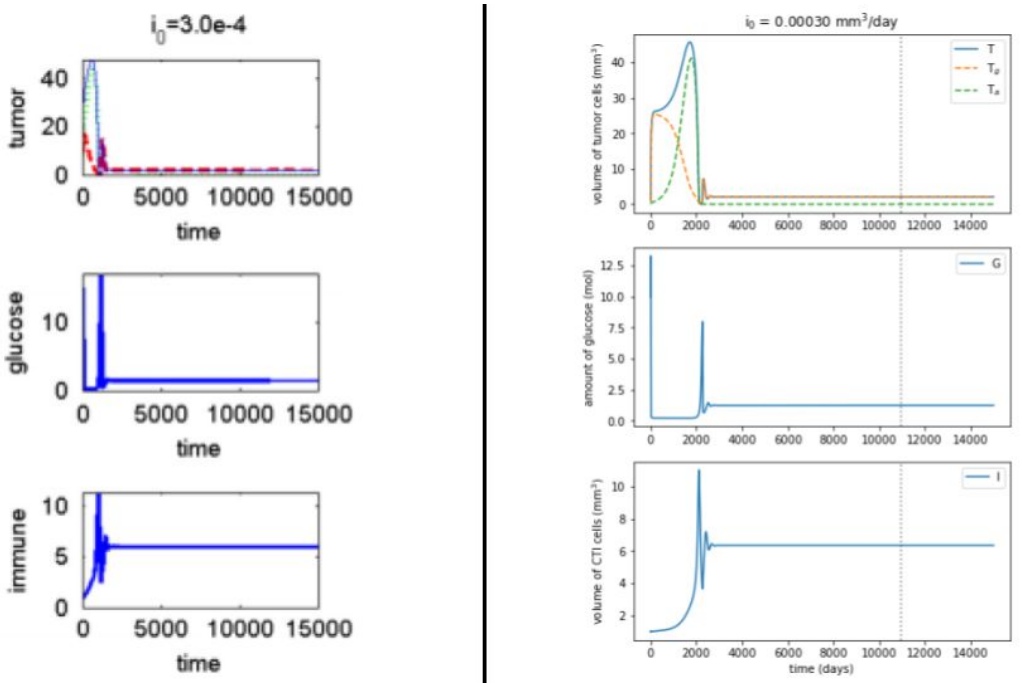


Figure 10. Results of simulation with $i_0 = 0.00030$ mm$^3$/day [1]

In this case, the immune response is sufficient to eliminate the tumor and prevent its relapse. All the species in the simulation stabilize at fixed values. This may be representative of a positive clinical outcome in which the tumor, while not eliminated, remains low in size.

**Simulating the Effects of Chemotherapeutic Intervention**

Further increase of the immune stimulus did not result in further reduction of tumor size, suggesting that metabolic competition from the immune system may not be sufficient to eliminate the tumor. Chemotherapy is often used in conjunction with immunotherapy to supplement treatment [9]. However, since nonspecific chemotherapy can affect the population of immune cells, there arises a possibility that the favorable balance achieved in the previous simulation can be disrupted.

To explore the effects of chemotherapeutic interventions on the microenvironment, simulations were carried out with the revised set of equations outlined in Figure 6. The value of $i_0$ was maintained at 0.00030 $mm^3$/day since it previously induced the 'elimination' phase of immunoediting. The administration of the dose was introduced as an event on the 4,000$^{th}$ day, which occurs after the populations have stabilized.

The results of a parameter scan that varied the magnitude of the chemotherapeutic dose showed that certain doses could disrupt the favorable stability previously achieved (Figure 11).

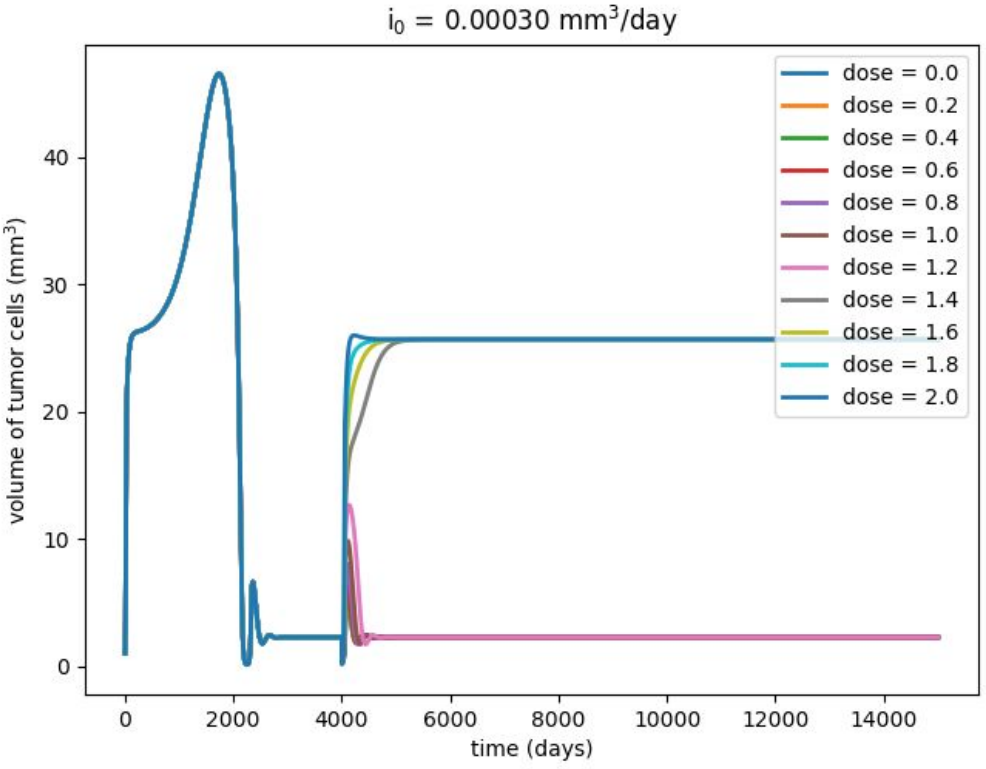


Figure 11. Parameter scan of doses administered at time = 4000 days

Comparing the results of different doses (Figure 12), it appears that the tumor cell population and the immune cell population are both negatively affected by the chemotherapeutic dose, but a low dose allows the immune system to recover and bring tumor growth under control, while a higher dose allows the glycolytic tumor cells to circumvent the immunoediting process.

Focusing on the point of administration allows a more detailed evaluation of the dose's effect (Figure 13). At a low dose, the tumor is almost eliminated by the chemotherapy. The population of immune cells is reduced as well. The resultant rise in glucose promotes the growth of glycolytic cells. However, the recovering population of immune cells,

stimulated by the increase in tumor size as well as the presence of glucose, inhibits the growth of the tumor before it can enter the ‘escape’ phase.

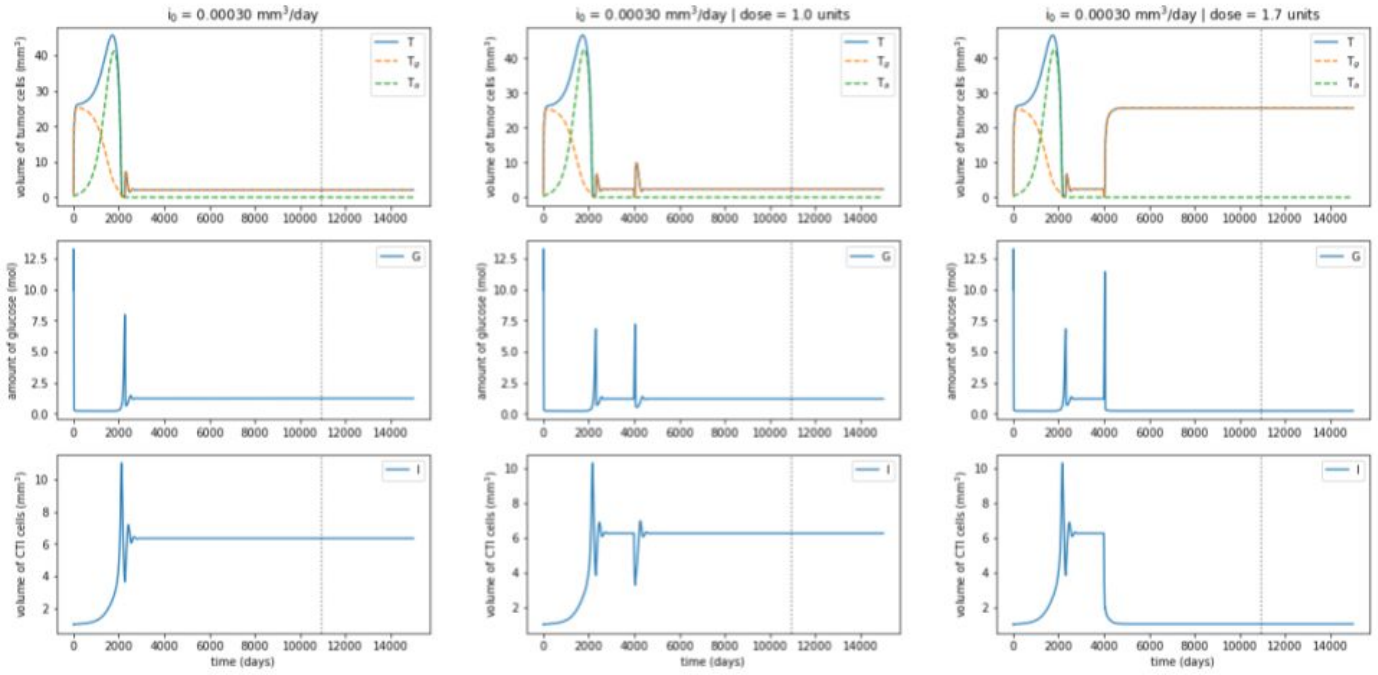


Figure 12. Comparison of outcomes with (a) no dose (b) dose = 1.0 units (c) dose = 1.7 units

At a high dose, however, the immune cell population fails to recover before the glycolytic tumor cell population ‘escapes’. Inhibited by a scarcity of glucose in the microenvironment, $I$ stabilizes at a low non-zero value, allowing $T_g$ to maximize its value.

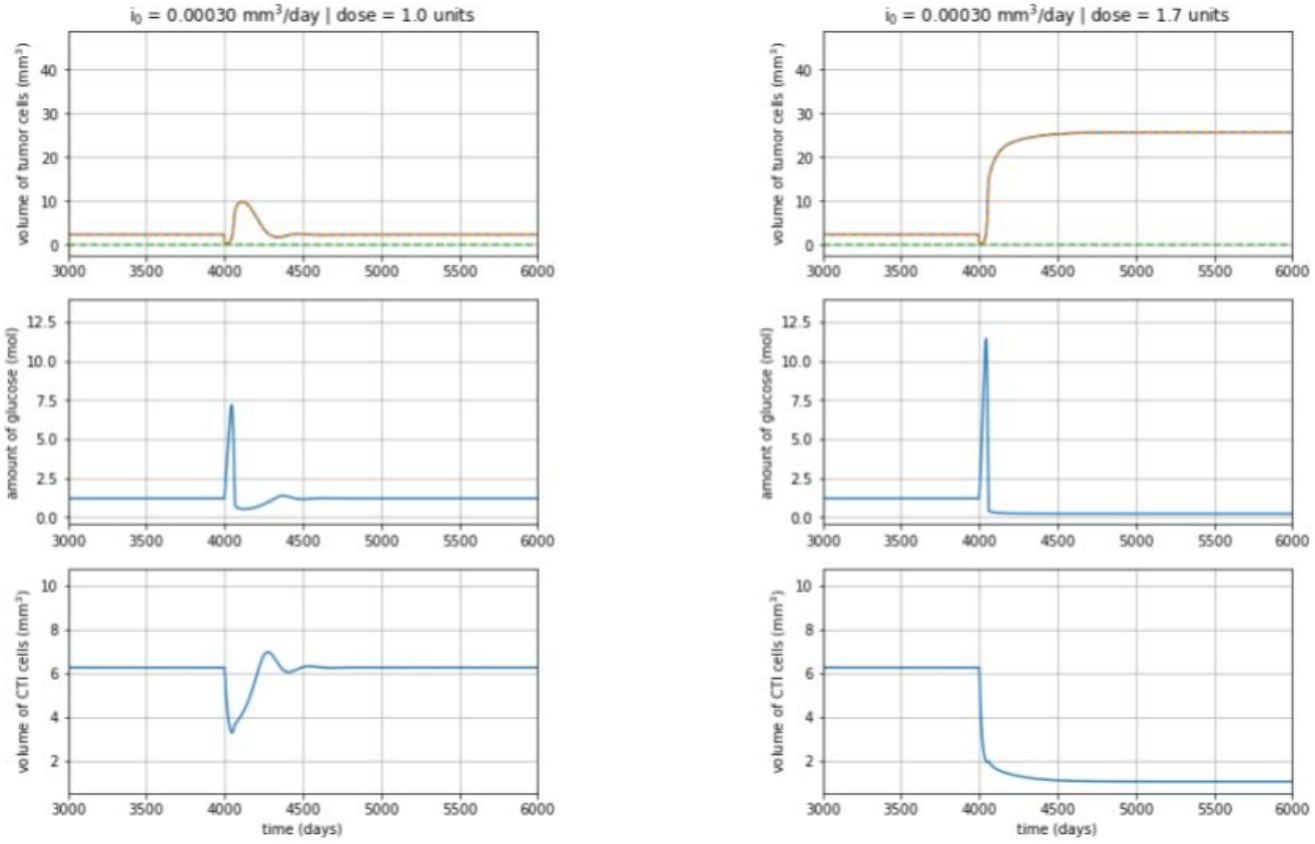


Figure 13. Result of intervention with (a) dose = 1.0 units (b) dose = 1.7 units

# Discussion

The results of the computational simulations support the hypothesis that metabolic competition can account for changes in the immunoediting process. Additionally, the model also supports the hypothesis that chemotherapeutic interventions can disrupt the stability of a favorable immunoediting phase.

## Clinical Significance

If the predictions of the model are experimentally validated, there may be a case for using immunostimulants to restrict cancerous growths to low sizes and therapeutically mitigate physiological effects rather than attempt a complete elimination of the tumor with chemotherapy and, as a result, possibly disrupt the immunoediting process.

The minor rise in tumor size prior to its subsequent reduction in Figure 10 may imply that, in certain medical cases, a rise in tumor size over a period of months may be temporary. Conversely, the high-amplitude oscillations in tumor size seen in Figure 9 may imply that near-elimination of a tumor can also be temporary.

Moreover, the significant role of glucose as a promoter of tumor cell populations may serve to fortify the case for carbohydrate restriction during the treatment of cancer [10].

## Prospects

A natural progression for the model's development is the incorporation of other factors that modulate the immunoediting process, such as the availability of oxygen at the tumor site. Accounting for the permeating effects of lactic acid that can aid cancer metastasis would also lead to a more accurate model.

Considering the critical role that glucose seems to play in the immunoediting process, it would be prudent to explore the effect of fluctuations in blood glucose levels, as exhibited by diabetic patients. Such a model would require the consolidation of two different time scales, with glucose levels fluctuating over the course of hours as a result of daily behavior, as well as over days as a result of the immunoediting process.

## Conclusion

If the above model is expanded to account for an adequate set of factors and subsequently experimentally validated, the model may be leveraged as a form of personalized medicine. In an ideal scenario, healthcare providers could populate the model's parameters by collecting data from individual patients and simulating various treatments by optimizing parameters that can be controlled in practice. Despite the possibility that a perfectly accurate model may not emerge in practice, partly due to the variations in biological parameters induced by mutations, the results of the model's simulations may be considered as a supplement to conventional methods of planning oncological treatments.

# Appendix: Parameters

The parameters in the model were initialized using the values specified by Kareva and Berezovskaya (Table 1).

**Table 1**
Variables and parameters used in Eq. (1). Due to the form in which data was available, we chose to cast $G(t)$ in the units of moles as opposed to volume; the values of parameters that compare dynamics of aerobic as compared to glycolytic cells were taken based on theoretical considerations and citations.

| | Description | Estimated value | Units |
|---|---|---|---|
| $T(t)$ | population of tumor cells, composed of aerobic $T_a(t)$ and glycolytic $T_g(t)$ cells | $T(t) \geq 0$ | vol |
| $G(t)$ | glucose | $G(t) \geq 0$ | moles |
| $I(t)$ | cytotoxic immune cells | $I(t) \geq 0$ | vol |
| $r_a$ | growth rate of aerobic cancer cells | $4.31 \times 10^{-1}$ | 1/day |
| $r_g$ | growth rate of glycolytic cancer cells | $r_a \times k_1, k_1 \in [0.5, 5.0]$ | 1/day |
| $\mu_a$ | natural death rate or aerobic cancer cells | 0.01 | 1/day |
| $\mu_g$ | natural death rate of glycolytic cancer cells | $\mu_g \times k_2, k_2 \in [1.0, 10.0]$ | 1/day |
| $e_a$ | fractional aerobic cell kill by immune cells | 0.1 | 1/day |
| $e_g$ | fractional glycolytic cell kill by immune cells | $e_a - k_3, k_3 \in [-0.1, 0.1]$ | 1/day |
| $s$ | steepness coefficient of the tumor cell kill by immune cells | $6.18 \times 10^{-1}$ | n/a |
| $b_T$ | steepness coefficient for glucose-dependent growth of tumor cells | 0.9 | n/a |
| $b_I$ | steepness coefficient for glucose-dependent growth of immune cells | 0.9 | n/a |
| $G_0$ | rate of glucose inflow into tumor microenvironment from the blood stream | $G_0 \in [0.01, 2.06]$ | mol/day |
| $\mu_G$ | rate of glucose outflow from tumor microenvironment from blood stream | 0.01 | 1/day |
| $d_a$ | rate of glucose consumption by aerobic tumor cells | $d_a \in [0.048, 0.5]$ | mol/vol/day |
| $d_g$ | rate of glucose consumption by glycolytic tumor cells | $d_g \in [.1268, 0.5262]$ | mol/vol/day |
| $d_I$ | rate of glucose consumption by actively proliferating immune cells | $d_I \approx d_g$ | mol/vol/day |
| $i_0$ | rate of tumor-stimulated inflow of immune cells | $i_0 \in [0.001, 0.100]$ | vol/day |
| $\mu_I$ | natural death rate of cytotoxic immune cells | $2.0 \times 10^{-2}$ | 1/day |
| $r_I$ | rate at which immune cells are stimulated to be produced as a result of coming in contact with tumor debris from previously killed tumor cells | $3.03 \times 10^{-1}$ | 1/vol/day |
| $\xi_I, \xi_T$ | saturation coefficient for glucose-dependent immune and tumor growth | 1 | moles |

Table 1. Variables and parameters used by Kareva and Berezovskaya [1]

For the modified model, the decay rate ($\mu_C$) of the chemotherapeutic species ($C$) was set as 1 unit/day. The composited immune cell elimination rate ($\mu_{Ic}$) was initialized to the value of the natural immune cell elimination rate ($\mu_I$). Coefficient $k_I$ was assigned a value of 100 mm$^3$. The percentage of tumor cells eliminated by chemotherapy was assumed to be 90%. Additionally, the recovery period of the immune cells ($p$) was set at 28 days [11].

# References

[1]I. Kareva and F. Berezovskaya, "Cancer immunoediting: A process driven by metabolic competition as a predator–prey–shared resource type model", Journal of Theoretical Biology, vol. 380, pp. 463-472, 2015.

[2]L. Ferreira, "Cancer metabolism: The Warburg effect today", Experimental and Molecular Pathology, vol. 89, no. 3, pp. 372-380, 2010.

[3]M. Liberti and J. Locasale, "The Warburg Effect: How Does it Benefit Cancer Cells?", Trends in Biochemical Sciences, vol. 41, no. 3, pp. 211-218, 2016.

[4]D. Ngo, K. Ververis, S. Tortorella and T. Karagiannis, "Introduction to the molecular basis of cancer metabolism and the Warburg effect", Molecular Biology Reports, vol. 42, no. 4, pp. 819-823, 2015.

[5]R. Strausberg, "Tumor microenvironments, the immune system and cancer survival", Genome Biology, vol. 6, no. 3, p. 211, 2005.

[6]D. Mittal, M. Gubin, R. Schreiber and M. Smyth, "New insights into cancer immunoediting and its three component phases—elimination, equilibrium and escape", Current Opinion in Immunology, vol. 27, pp. 16-25, 2014.

[7]"Cancer of Any Site - Cancer Stat Facts", National Cancer Institute. [Online]. Available: https://seer.cancer.gov/statfacts/html/all.html. [Accessed: 08- Dec- 2018].

[8]"Life expectancy at birth, total (years) | Data", The World Bank. [Online]. Available: https://data.worldbank.org/indicator/SP.DYN.LE00.IN. [Accessed: 08- Dec- 2018].

[9]"Understanding Immunotherapy", Cancer.Net, 2018. [Online]. Available: https://www.cancer.net/navigating-cancer-care/how-cancer-treated/immunotherapy-and-vaccines/understanding-immunotherapy. [Accessed: 08- Dec- 2018].

[10]R. Klement and U. Kämmerer, "Is there a role for carbohydrate restriction in the treatment and prevention of cancer?", Nutrition & Metabolism, vol. 8, no. 1, p. 75, 2011.

[11]"How Chemotherapy Affects the Immune System", Breastcancer.org, 2014. [Online]. Available: https://www.breastcancer.org/tips/immune/cancer/chemo. [Accessed: 08- Dec- 2018].